IMPRESSIVE FREQUENCY BEHAVIOR OF RAYLEIGH HYPER-ELASTIC MICRO-BEAM IN COMPARISION WITH EULER-BERNOULLI THEORY

Saeed DANAEE BARFOROOSHI[1], Ardeshir KARAMI MOHAMMADI[2]

Hyper-elastic micro-beam that is sandwiched between two compliant electrodes is considered here. The hyper-elastic behavior is introduced by Yeoh model and von-Karman strain-displacement relationship is used to consider geometric nonlinearity. Governing equation is derived based on Rayleigh beam theory, and Lindstedt-Poincare method is the solution procedure. The results are compared with Euler-Bernoulli beam theory and show different behavior of hyper-elastic beam from usual beams. In addition, the effects of some parameters are studied on nonlinear frequency.

Keywords: Rayleigh, Euler-Bernoulli, Yeoh, hyper-elastic.

1. Introduction

Dielectric elastomers are particular class of electro-active polymers that have received a great deal of attention recently. They have high-energy output, large strains, outstanding combination of flexibility, low cost and chemical, simplicity of structure and robustness due to the use of stable and commercially available polymer materials [1-3]. These properties make dielectric elastomers as a first-rate candidate for applications such as artificial muscles, sensors, generators, loudspeakers, micro air vehicles, energy harvesting, actuators and resonators [4-5]. Dielectric elastomer as a hyperelastic and rubber material includes material nonlinearity and it should be modeled correctly. Few articles are reported in accounting this property and majority of them deal with only geometric nonlinearity. Mason and Maluleke [6] derived three non-linear differential equations for radial oscillations in radial, tangential and longitudinal transversely isotropic thin-walled cylindrical tubes of generalized Mooney–Rivlin material. They reduced radial and tangential transversely isotropic tubes differential equations to Abel equations of the second kind. Verron et al [7] analyzed dynamic inflation of hyperelastic spherical membranes of a Mooney–

[1] PhD candidate., Dept. of Mechanical Engineering, SHAHROOD University of Technology, Iran, e-mail: saeeddanaee@gmail.com
[2] Associate Prof., Dept. of Mechanical Engineering, SHAHROOD University of Technology, Iran, e-mail: akaramim@yahoo.com

Rivlin material. In addition, they examined the conditions for oscillatory inflation around the static fixed point and found that, for a given material, the frequency of oscillation exhibits a maximum at some pressure level, which tends to increase for materials closer to neo-Hookean behavior. Ogden and Roxburgh [8] studied plane incremental vibrations superimposed on the pure homogeneous deformation of a rectangular block of incompressible isotropic elastic material. They obtained frequency equations, which determine the frequencies of symmetric and anti-symmetric modes of vibration in respect of a general form of strain-energy function. The plate that was their case study had rectangular shape and it was assumed incompressible, so the third strain invariant was equal to one in their formulation. . Karami mohammadi and Danaee Barforooshi [9] Studied nonlinear forced vibration of dielectric elastomer micro-beam. They used Yeoh hyper-elastic model to include material nonlinearity beside geometric nonlinearity. They showed that micro-beam with Yeoh model has hardening behavior. In addition they showed direct effect of force amplitude and mode number on hardening behavior of hyper-elastic micro-beam. Zhu et al. [10] analyzed a membrane of a dielectric elastomer, prestretched and mounted on a rigid circular ring. They showed that the natural frequencies of dielectric elastomers are tunable by varying the prestretch, pressure, or voltage, when driven by a sinusoidal voltage. Also, superharmonic, harmonic and subharmonic responses were founded in their analysis.

Danaee Barforooshi and Karami Mohammadi [11] considered a micro-bridge resonator with geometric and material nonlinearity. Geometric nonlinearities were introduced by von-Karman and for material nonlinearity; the Yeoh and neo-Hookean models were used. They showed that neo-Hookean model is not suitable for this case, because of insufficient terms in its strain-energy function. They used perturbation technique for solution of nonlinear governing equation and achieved good agreement between analytical and numerical method. They showed the significant influence of mode number on normalized frequency so that the higher the mode number, the more the influence of aspect ratio.

In this article, another suitable hyper-elastic model is used to study dielectric-elastomer microbeam behavior. In addition to study the behavior of system based on Rayleigh theory, a comparison of linear and nonlinear frequency will be done between this theory and Euler-Bernoulli theory.

2. Governing equation based on Rayleigh theory

In this section, governing equation of free vibration of hyper-elastic micro-beam will be derived. As it is shown in Fig.1, elastomer-based beam has uniform thickness d , length L , width b and density ρ.

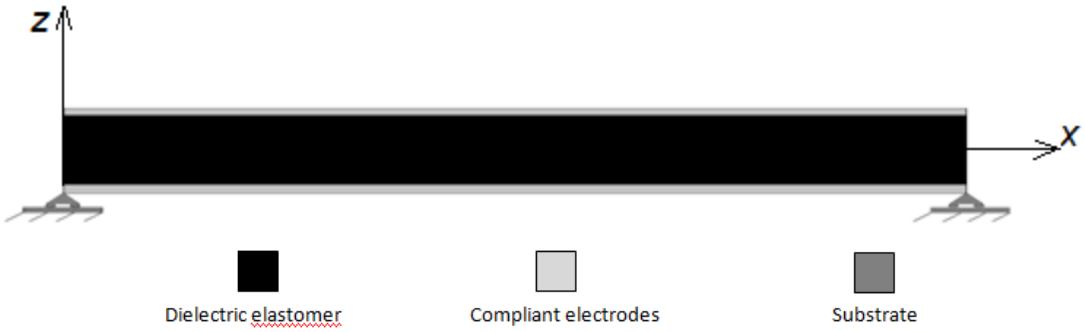

Fig. 1. Schematic of hyper-elastic DE micro-beam

As we know, rotary inertia is included in Rayleigh's theory. The reason is that since the cross section remains plane during motion, the axial motion of points located in any cross section undergoes rotary motion about the y axis [12].

$$u = -z\frac{\partial w(x,t)}{\partial x}, \quad v = 0, \quad w = w(x,t) \tag{1}$$

where u is the axial displacement of the centroid of the sections along Ox and w denotes the lateral deflection of the beam along Oz. $\frac{\partial w(x,t)}{\partial x}$ stands for the angle of rotation of the beam cross section about y-axis.

According to large deformation, we cannot use classic strain tensor and Green-Lagrange strain deformation is a good choice.

$$\varepsilon_{ij} = \frac{1}{2}\left(\frac{\partial u_i}{\partial x_j} + \frac{\partial u_j}{\partial x_i} + \frac{\partial u_k}{\partial x_j}\frac{\partial u_k}{\partial x_i}\right) \tag{2}$$

In accordance with equation (2), strain components are:

$$\begin{aligned} \varepsilon_{11} &\approx -z\frac{\partial^2 w}{\partial x^2} + \frac{1}{2}\left(\frac{\partial w}{\partial x}\right)^2 \\ \varepsilon_{13} &= \varepsilon_{31} = \varepsilon_{33} \approx 0 \\ \varepsilon_{12} &= \varepsilon_{21} = \varepsilon_{22} = \varepsilon_{23} = \varepsilon_{32} = 0 \end{aligned} \tag{3}$$

For deriving equation of motion in free vibration via Hamiltonian principle, we need kinetic and potential energy that are as follows, respectively:

$$T = \frac{1}{2}\int_0^l \rho A\left(\frac{\partial w}{\partial t}\right)^2 dx \tag{4}$$

$$\Pi = \int_V W dV \tag{5}$$

Yeoh developed a hyper-elastic material model that only depends on the first strain invariants. This model is based on a series expansion and its series is truncated after the first three terms. Therefore, its strain energy density function is:

$$W = \sum_{i=1}^{3} c_i \, (\mathrm{I}_1 - 3)^i \tag{6}$$

Where c_i are material constants and I_1 is the first strain invariant that is related to principle stretches and right Cauchy- Green strain tensor as follows:

$$I_1 = {\lambda_1}^2 + {\lambda_2}^2 + {\lambda_3}^2 = tr(\mathrm{C}) \tag{7}$$

It should be mentioned that $\lambda_i \; (i = 1, 2, 3)$ are square root of the right Cauchy- Green strain tensor (C) and C is related to strain tensor that its components introduced in equation (3).

$$C = 2E + I \tag{8}$$

Substituting equations (4) and (5) into Lagrange equation and applying Hamilton principle, leads to following governing equations:

$$\begin{aligned} &\rho A \frac{\partial^2 w}{\partial t^2} - \rho I \frac{\partial^4 w}{\partial x^2 \partial t^2} - 2c_1 A \frac{\partial^2 w}{\partial x^2} + 8c_2 I \frac{\partial^4 w}{\partial x^4} - 30c_3 A \frac{\partial^2 w}{\partial x^2}\left(\frac{\partial w}{\partial x}\right)^4 + 24c_3 I \left(\frac{\partial^2 w}{\partial x^2}\right)^3 \\ &+96c_3 I \frac{\partial^3 w}{\partial x^3}\frac{\partial^2 w}{\partial x^2}\frac{\partial w}{\partial x} + 24c_3 I \frac{\partial^4 w}{\partial x^4}\left(\frac{\partial w}{\partial x}\right)^2 - 12c_2 A \frac{\partial^2 w}{\partial x^2}\left(\frac{\partial w}{\partial x}\right)^2 = 0 \end{aligned} \tag{9}$$

with boundary conditions $w(0) = 0,\; w(\mathrm{L}) = 0,\; \frac{\partial^2 w}{\partial x^2}(0) = 0,\; \frac{\partial^2 w}{\partial x^2}(\mathrm{L}) = 0$.

Equation of motion and boundary conditions can be normalized with proper non-dimensional parameters:

$$x^* = \frac{x}{l}, \quad w^* = \frac{w}{d}, \quad t^* = t\omega_{\dim} \tag{10}$$

$\omega_{\dim}$ is the linear dimensional natural frequency of micro-beam that is achieved by linearization of equation (9).
Therefore, we have:

$$\begin{aligned} &\frac{\partial^2 w^*}{\partial t^{*^2}} - \alpha_1 \frac{\partial^4 w^*}{\partial x^{*^2} \partial t^{*^2}} - \alpha_2 \frac{\partial^2 w^*}{\partial x^{*^2}} + \alpha_3 \frac{\partial^4 w^*}{\partial x^{*^4}} - \alpha_4 \frac{\partial^2 w^*}{\partial x^{*^2}}\left(\frac{\partial w^*}{\partial x^*}\right)^4 + \alpha_5 \left(\frac{\partial^2 w^*}{\partial x^{*^2}}\right)^3 \\ &+4\alpha_5 \frac{\partial^3 w^*}{\partial x^{*^3}}\frac{\partial^2 w^*}{\partial x^{*^2}}\frac{\partial w^*}{\partial x^*} + \alpha_5 \frac{\partial^4 w^*}{\partial x^{*^4}}\left(\frac{\partial w^*}{\partial x^*}\right)^2 - \alpha_6 \frac{\partial^2 w^*}{\partial x^{*^2}}\left(\frac{\partial w^*}{\partial x^*}\right)^2 = 0 \end{aligned} \tag{11}$$

that

$$\alpha_1 = \frac{I}{l^2 A} \quad \alpha_2 = \frac{2c_1}{\rho l^2 \omega_{\dim}^2} \quad \alpha_3 = \frac{8c_2 I}{\rho A l^4 \omega_{\dim}^2}$$
$$\alpha_4 = \frac{30c_3 d^4}{\rho l^6 \omega_{\dim}^2} \quad \alpha_5 = \frac{24c_3 I d^2}{\rho A l^6 \omega_{\dim}^2} \quad \alpha_6 = \frac{12c_2 d^2}{\rho l^4 \omega_{\dim}^2} \tag{12}$$

with normalized boundary conditions $w^*(0) = 0,\ w^*(1) = 0,\ \frac{\partial^2 w^*}{\partial x^{*2}}(0) = 0,\ \frac{\partial^2 w^*}{\partial x^{*2}}(1) = 0$.

3. Lindstedt-Poincare method

In accordance with Lindstedt-Poincare technique, small perturbation parameter and time transformations are introduced by $w^* = \varepsilon\eta$ and $\tau = \omega t^*$ respectively. So Eq. (11) in free vibration form will be:

$$\omega^2 \varepsilon \frac{\partial^2 \eta}{\partial \tau^2} - \alpha_1 \varepsilon \omega^2 \frac{\partial^4 \eta}{\partial x^2 \partial t^2} - \alpha_2 \varepsilon \frac{\partial^2 \eta}{\partial x^2} + \alpha_3 \varepsilon \frac{\partial^4 \eta}{\partial x^4}$$
$$-\alpha_4 \varepsilon^5 \frac{\partial^2 \eta}{\partial x^2}\left(\frac{\partial \eta}{\partial x}\right)^4 + \alpha_5 \varepsilon^3 \left(\frac{\partial^2 \eta}{\partial x^2}\right)^3 + 4\alpha_5 \varepsilon^3 \frac{\partial^3 \eta}{\partial x^3}\frac{\partial^2 \eta}{\partial x^2}\frac{\partial \eta}{\partial x} \tag{13}$$
$$+\alpha_5 \varepsilon^3 \frac{\partial^4 \eta}{\partial x^4}\left(\frac{\partial \eta}{\partial x}\right)^2 - \alpha_6 \varepsilon^3 \frac{\partial^2 \eta}{\partial x^2}\left(\frac{\partial \eta}{\partial x}\right)^2 = 0$$

Both the non-dimensional deflection and frequency can be expanded into series forms as:

$$\eta = \eta_0(x^*, \tau) + \varepsilon\eta_1(x^*, \tau) + \varepsilon^2\eta_2(x^*, \tau) + \ldots \tag{14-1}$$
$$\omega = \omega_0 + \varepsilon\omega_1 + \varepsilon^2\omega_2 + \ldots \tag{14-2}$$

that ω_0 is the frequency of linear governing equation.

Calculating linear frequency (ω_0) is exactly as the procedure in section 3, but the equation is:

$$\omega^2 \varepsilon \frac{\partial^2 \eta}{\partial \tau^2} - \alpha_1 \varepsilon \omega^2 \frac{\partial^4 \eta}{\partial x^2 \partial t^2} - \alpha_2 \varepsilon \frac{\partial^2 \eta}{\partial x^2} + \alpha_3 \varepsilon \frac{\partial^4 \eta}{\partial x^4} = 0 \tag{15}$$

So the linear non-dimensional frequency will be:

$$\omega_0^2 = \frac{n^2\pi^2(\alpha_2 + \alpha_3 n^2 \pi^2)}{1 + \alpha_1 n^2 \pi^2} \tag{16}$$

Substituting Eqs. (14) into Eq. (13) and arranging them, based on different orders of ε_i, one has the following perturbation equations:

$$\varepsilon^1 :\ \omega_0^2 \frac{\partial^2 \eta_0}{\partial \tau^2} - \alpha_2 \frac{\partial^2 \eta_0}{\partial x^2} - \alpha_1 \omega_0^2 \frac{\partial^4 \eta_0}{\partial x^2 \partial \tau^2} + \alpha_3 \frac{\partial^4 \eta_0}{\partial x^4} = 0 \tag{17}$$

$$\varepsilon^2 : \omega_0^2 \frac{\partial^2 \eta_1}{\partial \tau^2} - \alpha_2 \frac{\partial^2 \eta_1}{\partial x^2} + \alpha_3 \frac{\partial^4 \eta_1}{\partial x^4} - \alpha_1 \omega_0^2 \frac{\partial^4 \eta_1}{\partial x^2 \partial \tau^2} + 2\omega_0 \omega_1 \frac{\partial^2 \eta_0}{\partial \tau^2} - 2\alpha_1 \omega_0 \omega_1 \frac{\partial^4 \eta_0}{\partial x^2 \partial \tau^2} = 0 \tag{18}$$

$$\begin{aligned} \varepsilon^3 : & \omega_0^2 \frac{\partial^2 \eta_2}{\partial \tau^2} - \alpha_2 \frac{\partial^2 \eta_2}{\partial x^2} - (2\omega_0 \omega_2 + \omega_1^2) \frac{\partial^4 \eta_0}{\partial x^2 \partial \tau^2} \\ & + 2\alpha_1 \omega_0 \omega_1 \frac{\partial^4 \eta_1}{\partial x^2 \partial \tau^2} - \alpha_1 \omega_0^2 \frac{\partial^4 \eta_2}{\partial x^2 \partial \tau^2} + \alpha_3 \left(\frac{\partial^4 \eta_2}{\partial x^4} \right) \\ & + 2\omega_0 \omega_1 \frac{\partial^2 \eta_1}{\partial \tau^2} + (2\omega_0 \omega_2 + \omega_1^2) \frac{\partial^2 \eta_0}{\partial \tau^2} + \alpha_5 \left(\frac{\partial^4 \eta_0}{\partial x^4} \right) \left(\frac{\partial \eta_0}{\partial x} \right)^2 \\ & + 4\alpha_5 \left(\frac{\partial^3 \eta_0}{\partial x^3} \right) \left(\frac{\partial^2 \eta_0}{\partial x^2} \right) \left(\frac{\partial \eta_0}{\partial x} \right) + \alpha_5 \left(\frac{\partial^2 \eta_0}{\partial x^{*2}} \right)^3 - \alpha_6 \left(\frac{\partial^2 \eta_0}{\partial x^2} \right) \left(\frac{\partial \eta_0}{\partial x} \right)^2 = 0 \end{aligned} \tag{19}$$

Deflection function in each of these equations can be expressed as the products of two separated functions:

$$\eta_{im}(\mathrm{x}^*, \mathrm{t}) = \mathrm{T}_{im}(\tau)\, \mathrm{U}_{im}(\mathrm{x}^*) \quad i = 0,1,2 \qquad \mathrm{U}_{im}(\mathrm{x}^*) = \sqrt{2} \sin(\mathrm{n}\, \pi\, \mathrm{x}) \tag{20}$$

in which $\mathrm{U}_{\mathrm{im}}(\mathrm{x}^*)$ is the trial function of the simply-supported micro-beam[19].

Substituting Eq. (20) into Eqs. (17), (18) and (19) and then applying the Galerkin method, the so-called PDE will be reduced to ODE and then it can be solved. It should be mentioned that the initial conditions are $T(0) = \tilde{A}_{\max}$, $\dot{T}(0) = 0$. $\tilde{A}_{\max}$ is the maximum normalized amplitude of deflection that $\tilde{A}_{\max} = \frac{A_{\max}}{d}$.

Solution of equation (20) is:

$$\eta_0 = \sqrt{2} \sin(\mathrm{n}\, \pi\, \mathrm{x})\, \tilde{\mathrm{A}}_{\max} \cos(\sqrt{\beta}\tau) \tag{21}$$

that

$$\beta = \frac{\mathrm{n}^2 \pi^2 (\alpha_2 + \alpha_3 \mathrm{n}^2 \pi^2)}{\omega_0^2 (1 + \alpha_1 \mathrm{n}^2 \pi^2)} \tag{22}$$

Solution of equation (18) is:

$$\eta_1 = 0 \tag{23}$$

Eliminating the terms that leads to secular terms, will give:

$$\omega_1 = 0 \tag{24}$$

Solution of equation (19) is:

$$\eta_2 = \sqrt{2}\, \frac{\gamma}{\beta} \sin(\mathrm{n}\, \pi\, \mathrm{x}) \cos(3\sqrt{\beta_1}\tau) \tag{25}$$

that

$$\gamma = \frac{A_{\max}^3 n^4 \pi^4 (\alpha_6 + 2\alpha_5 n^2 \pi^2)}{\omega_0^2 (1 + \alpha_1 n^2 \pi^2)} \tag{26}$$

Eliminating the terms that leads to secular terms, will give:

$$\omega_2 = \frac{\tilde{A}_{\max}^2 n^4 \pi^4 (\alpha_6 + 2\alpha_5 n^2 \pi^2)}{\omega_0 \beta (1 + \alpha_1 n^2 \pi^2)} \tag{27}$$

Total deflection response of the micro-resonator is the sum of all of the above solutions.

After applying the transformation $w^* = \varepsilon\eta$ final solution will be:

$$w^* = \sum_{m=1}^{\infty} \varepsilon\eta_{0m}(x^*, \tau) + \varepsilon^2 \eta_{1m}(x^*, \tau) + \varepsilon^3 \eta_{2m}(x^*, \tau) \tag{28}$$

4. Numerical results and comparison with Euler-Bernoulli theory

For discussing about frequency curves, we use geometrical and material properties. For this purposes we introduce geometrical and material properties in table 1. Material constants are based on uni-axial tension test [13].

Table 1

Micro-beam geometrical and material properties

Geometric properties	Material properties
$l = 30\mu m$ $b = 10\mu m$ $d = 3\mu m$	$c_1 = 0.24162\,MPa$ $c_2 = 0.19977\,MPa$ $c_3 = -0.00541 MPa$

At the first step, we survey the effect of length on frequency curves. The length of the beam is considered from $30\,\mu m$ to $100\,\mu m$. It should be mentioned that the thickness of the beam will be constant as wrote in table one. Maximum amplitude is considered as 0.6 of the thickness.

The Fig. 2 shows the effect of beam length on nonlinear frequency at the first three modes.

As it is seen, in all modes the frequency decreases as larger lengths are considered and tends to linear frequency. In addition, the rate of change is bigger in higher modes. Comparison of frequency in these modes shows that quantity of frequency is larger at higher modes.

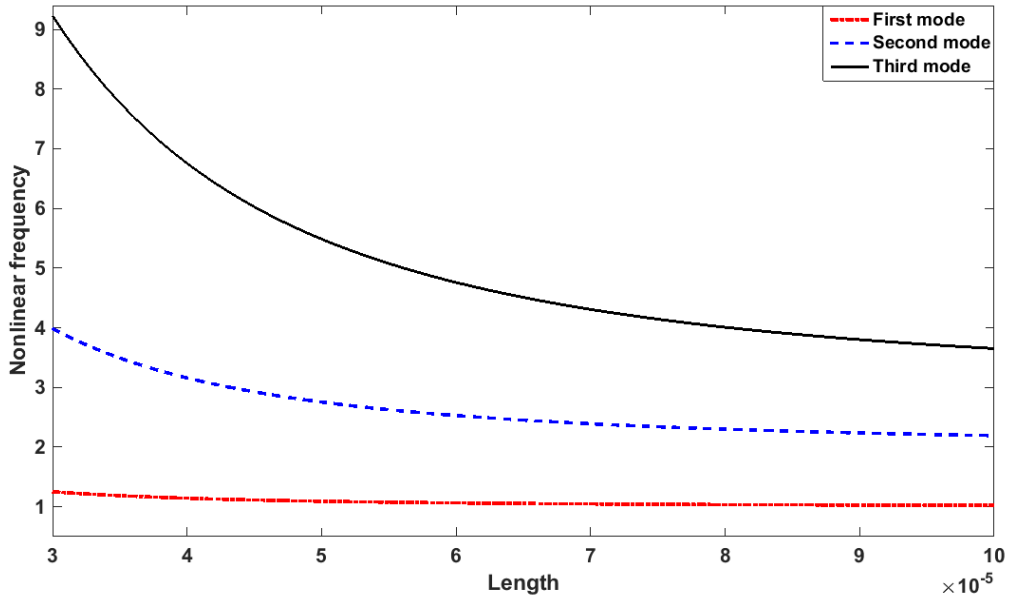

Figure2. Effect of beam length on nonlinear frequency at the first three modes

Although the linear frequency (ω_0) achieved by Rayleigh and Euler-Bernoulli theory are so close to each other, but as it is expected the linear frequency predicted by Euler-Bernoulli is larger than Rayleigh one. These frequencies are presented in table 2 for the first three modes. It should be mentioned that the geometric properties are as table 1.

Table2

Comparison linear frequency in Rayleigh and Euler-Bernoulli theory

Mode number	Rayleigh	Euler-Bernoulli
n=1	0.9959	1
n=2	2.0446	2.0779
n=3	3.1867	3.3025

For nonlinear frequency, unlike the linear one, the quantity predicted by Rayleigh theory is larger than Euler-Bernoulli. This comparison is expressed for the first three modes in table 3.

Table3

Comparison nonlinear frequency in Rayleigh and Euler-Bernoulli theory

Mode number	Rayleigh	Euler-Bernoulli
n=1	1.2520	1.0321
n=2	2.3239	3.9877
n=3	9.2293	4.0790

This result is also shown in figure (3) for the first three modes. While the behavior of frequency is the same in both of theories but Rayleigh theory predicts larger nonlinear frequencies in all lengths and modes. It can be concluded from table 3 and figure (5) that the difference between two theories gets larger at higher modes. In this figure, R and E-B stand for Rayleigh and Euler-Bernoulli, respectively.

This is the outstanding different between ordinary and hyper-elastic beams and can be related to material nonlinearity characteristic that hyper-elastic beams show.

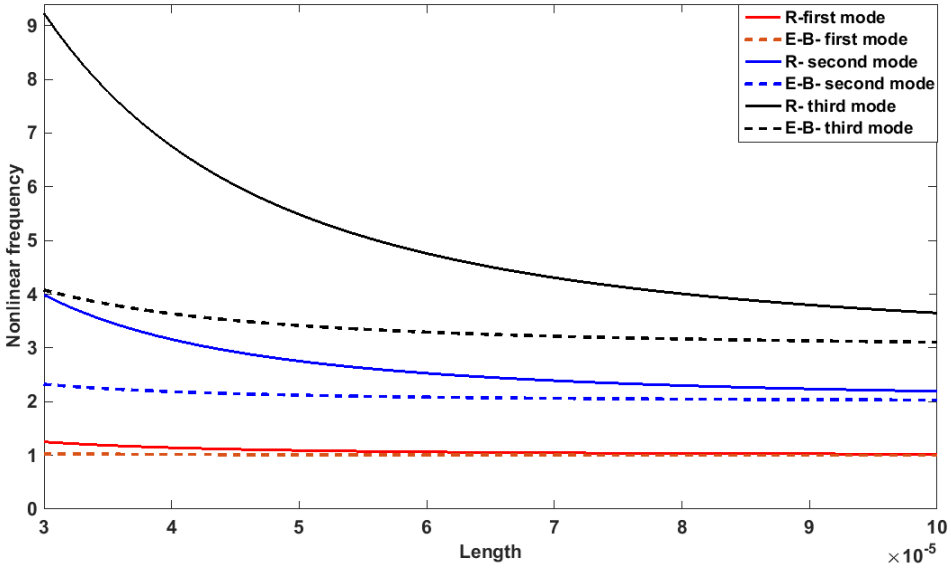

Figure 3. Comparison nonlinear frequency between Rayleigh and Euler-Bernoulli theories for the first three modes

Also it can be shown that the rate of nonlinear frequency difference, between Euler-Bernoulli and Rayleigh theories has a direct relationship with maximum amplitude of beam and inverse relationship with aspect ratio(L / d).

At the first step of comparison, we compare the latter results with the new maximum amplitude (0.8 of thickness).

Table4

Comparison nonlinear frequency in Rayleigh and Euler-Bernoulli theory with $w_{\max} = 0.8d$

Mode number	Rayleigh	Euler-Bernoulli
n=1	1.4512	1.0571
n=2	5.4990	2.5152
n=3	13.9291	4.6829

As it is obvious, quantity of nonlinear frequency, get larger in Rayleigh theory with increasing in maximum amplitude.

In addition, a comparison between the quantities in table 1 and new aspect ratio can be done. New geometrical properties are shown in table 5 so that the aspect ratio becomes smaller.

Table 5

New micro-beam aspect ratio

Geometric properties	Material properties
$l = 30\mu m$ $b = 10\mu m$ $d = 6\mu m$	$c_1 = 0.24162\,MPa$ $c_2 = 0.19977\,MPa$ $c_3 = -0.00541\,MPa$

Table 6 shows that nonlinear frequencies depicted by new smaller aspect ratio are larger in comparison with table 3. Also from table 4 and table 6 it can be concluded that the effect of aspect ratio on nonlinear frequency is more than maximum amplitude.

Table6

Comparison nonlinear frequency in Rayleigh and Euler-Bernoulli theory with $w_{\max} = 0.6d$

Mode number	Rayleigh	Euler-Bernoulli
n=1	1.9191	1.1184
n=2	8.3538	3.0898
n=3	19.9083	6.2629

5. Conclusions

Microbeam with dielectric elastomer sandwiched between two compliant electrodes was considered in this research. The boundary condition was simply-supported, so von-Karman strain-displacement relationship was used for geometric nonlinearity. Yeoh model was the suitable hyper-elastic model for involving material nonlinearity. Deriving equation was based on Rayleigh theory and influence of length of beam was studied on nonlinear frequency. As it was shown, the frequency decreases when the length get larger. In addition, a comparison between Rayleigh and Euler-Bernoulli theories was done. Results showed that the linear frequency predicted by Rayleigh theory is smaller than Euler-Bernoulli in all modes but nonlinear frequency is larger in Rayleigh theory and difference of predictions is more visible at higher modes. Also it was shown that the rate of nonlinear frequency difference, between Euler-Bernoulli and Rayleigh theories has a direct relationship with maximum amplitude of beam and inverse relationship with aspect ratio(L / d) so that the effect of aspect ratio as more.

R E F E R E N C E S

[1]. *Z. Suo*, "Theory of dielectric elastomers", Acta Mechanica Solida Sinica, **vol 23**, 2010, pp. 549-578.

[2]. *E. M. Mockensturm, N. Goulbourne*," Dynamic response of dielectric elastomers", International Journal of Non-Linear Mechanics, **vol 41**, 2006, 388 – 395.

[3]. *F. Carpi, D. De Rossi, R. Kornbluh, R.E. Pelrine, P. Sommer-Larsen*, Dielectric elastomers as electromechanical transducers: Fundamentals, materials, devices, models and applications of an emerging electroactive polymer technology, Elsevier,2011.

[4]. *H. Stoyanov,G. Kofod, R. Gerhard,* "A Co-Axial Dielectric elastomer actuator", Advance Science and Technology. **vol 61**, 2009, pp. 81–84.

[5]. *Y. Bar-Cohen*, Electroactive polymer (EAP) actuators as artificial muscles: reality, potential and challenges, SPIEPress, 2004.

[6]. *D.P. Mason, G.H. Maluleke*, "Non-linear radial oscillations of a transversely isotropic hyperelastic incompressible tube", Journal of Mathematical Analysis and Applications, 333, 2007, pp. 365–380.

[7]. *E. Verron, R.E. Khayat, A. Derdouri, B. Peseux*, "Dynamic inflation of hyperelastic spherical membrane", Journal of Rheology, **vol 43**, 1999, pp.1083-1097.

[8]. *R.W. Ogden, D.G. Roxburgh*, "The effect of pre-stress on the vibration and stability of elastic plates*".* International Journal of Engineering Science, **vol 31**, 1993, pp. 1611- 1639.

[9]. *A Karami Mohammadi, S. Danaee. Barforooshi*, "Nonlinear forced vibration analysis of dielectric-elastomer based micro-beam with considering Yeoh hyper-elastic model" Latin American Journal of Solids and Structures, **vol 14**, 2017**,** pp. 643-656.

[10]. *J. Zhu, S. Cai, Z. Suo*, "Resonant behavior of a membrane of a dielectric elastomer", International Journal of Solids and Structures, **vol 47**, 2010, pp. 3254–3262.

[11]. *S, Danaee. Barforooshi, A, Karami Mohammadi*, " study neo-Hookean and Yeoh hyper-elastic models in dielectric elastomer-based micro-beam resonators" Latin American Journal of Solids and Structures, **vol 13**, 2016, pp. 1823-1837.

[12]. *Rao.S.S*, vibration of continous systems, John Wiley and Sons, 2007.

[13]. *Martins, P. A. L. S. R, Natal Jorge, M, and Ferreira, A. J. M. A*. "Comparative Study of Several Material Models for Prediction of Hyperelastic Properties: Application to Silicone-Rubber and Soft Tissues", Strain Journal, **vol 42**, 2006, pp. 135-147.